Table III. Intermolecular Short Distances (Å)

O20(x, y, z)-O3B($1 + x, y, z$)	2.861
OC23(x, y, z)-W1($1 - x, \frac{1}{2} + y, 2 - z$)	2.986
O2A(x, y, z)-O4C($1 - x, y, 1 - z$)	2.774
O4C(x, y, z)-W1($1 + x, 1 + y, 1 + z$)	2.860
O3B-AC	3.052
O4B-AC	2.878

crown as shown by the ORTEP drawing and the torsion angle values (Table II).

B. Sugar Units. The configuration of the macrocycle being defined as above, the sugar units can be described as unit A, β-D-4,6-dideoxy-3-ketoallose; unit B, β-L-mycarose; unit C, β-D-mycinose.

C. Hydrogen Bonds, The two molecules of solvent in the cell (acetone and water) are linked to the sugar units by hydrogen bonds: acetone (AC) to unit B; water (W) to unit C (cf. Table III). There are no internal hydrogen bonds between the oxygen atoms of the macrocycle except perhaps between O3B-O4B (2.8 Å) (H(O3B)-O4B, 2.4 Å) and O20-O21 (2.6 Å) (H(O20)-O21, 2.4 Å); the two oxygen atoms are in the same plane (see Table III).

This work provides geometric data for the whole family of lankamycin-type antibiotics.

Supplementary Material Available: Listing of observed and calculated structural factors and the bond lengths and angles (20 pages). Ordering information is given on any current masthead page.

References and Notes

(1) (a) Institut de Chimie des Substances Naturelles. (b) Rhône-Poulenc Industries.
(2) French Patent 2 126 108 (Feb 25, 1971 and July 22, 1974, Société Rhône-Poulenc).
(3) (a) Hauptman, H.; Karle, J. *Acta Crystallogr.* **1956**, *9*, 635-651. (b) De Tita, G.; Edmonds, J. W.; Langs, D. A.; Hauptman, H. *Acta Crystallogr., Sect. A* **1975**, *31*, 472-479.
(4) Riche, C. *Acta Crystallogr., Sect. A* **1974**, *29*, 133-137.
(5) Riche, C., locally written program, 1978.
(6) Main, P. *Acta Crystallogr., Sect. A* **1977**, *33*, 750-757.
(7) Karle, J.; Karle I.L. *Acta Crystallogr.* **1966**, *21*, 849-859.
(8) (a) Keller-Schierlein, W.; Roncari, G. *Helv. Chim. Acta* **1964**, *47*, 78-103. (b) Egan, Richard S.; Martin, Jerry R. *J. Am. Chem. Soc.* **1970**, *92*, 4129-4130.
(9) Celmer, W. D. *J. Am. Chem. Soc.* **1965**, *87*, 1801-1802.

Iron–Ligand Stretching Band in the Resonance Raman Spectra of Ferrous Iron Porphyrin Derivatives. Importance as a Probe Band for Quaternary Structure of Hemoglobin

Hiroshi Hori and Teizo Kitagawa*

Contribution from the Department of Biophysical Engineering, Faculty of Engineering Science, Osaka University, Toyonaka, Osaka, 560, Japan, and the Institute for Protein Research, Osaka University, Suita, Osaka, 565, Japan.

Received November 1, 1979

Abstract: Resonance Raman spectra of ferrous iron picket-fence porphyrin [$Fe^{II}(T_{piv}PP)$] derivatives were observed for the oxy and deoxy states, both in solution and as a solid. The Fe(II)-N(2-MeIm) stretching mode of $Fe^{II}(T_{piv}PP)$(2-MeIm) was assigned by observing the frequency shifts upon the ^{54}Fe isotopic substitution (+3 cm^{-1}) and perdeuteration of 2-methylimidazole (2-MeIm) (−3 cm^{-1}). From the isotopic shifts the vibrational displacements of the Fe(II) ion and 2-MeIm perpendicular to the porphyrin plane were evaluated to be as large as 0.04_8 and 0.03_1 Å, respectively. For the iron protoporphyrin-2-methylimidazole complex [Fe^{II}(PP)(2-MeIm)], the Fe(II)-N(2-MeIm) stretching band was also observed at 206 cm^{-1} and identified by the deuteration shift (−3 cm^{-1}) of 2-MeIm. Consequently, our previous assignment of the quaternary structure-sensitive Raman line of deoxyhemoglobin to the Fe(II)-N_ϵ(His F8) stretching mode was confirmed. The Fe(II)-N(2-MeIm) stretching band of Fe^{II}(PP)(2-MeIm) was shifted from 206 to 220 cm^{-1} when detergent was absent. The frequency change was attributed to interactions between 2-MeIm and solvent H_2O, on the basis of the data for variation of the 2-MeIm/Fe^{II}(PP) ratio. The Fe(II)-O_2 stretching frequency differed appreciably between solution and solid state, but differed little between $Fe^{II}(T_{piv}PP)(1,2\text{-}Me_2Im)O_2$ and $Fe^{II}(T_{piv}PP)$(1-MeIm)O_2 even in the solid state, although the former and latter are considered to be models of the T and R structures of hemoglobin. The ν_4 frequencies of $Fe^{II}(T_{piv}PP)(1,2\text{-}Me_2Im)$ and $Fe^{II}(T_{piv}PP)$-(1-MeIm) in the solid state as well as in solution were distinct in the deoxy state, whereas they were alike in the oxy state. Thus, the oxygen affinity was presumed to be determined primarily in the deoxy state.

Analysis of resonance Raman spectra (RRS) of hemoproteins has provided detailed structural information on heme and its immediate surroundings.[1-3] Some Raman lines in the 1200-1700 cm^{-1} region have been practically used to characterize physicochemical properties of the heme of various hemoproteins including cytochrome P-450,[4,5] horseradish peroxidase,[6-8] cytochrome c',[9,10] and cytochrome oxidase.[11-14] Assignments of such Raman lines were discussed based mainly on the normal coordinate treatments.[15-19] A more complete set of experimental data including the isotopic frequency shifts, symmetry assignments, and combination modes has been collected for octaethylporphinatonickel(II) [Ni(OEP)],[20] and the vibrational modes for the individual Raman lines have been elucidated by the subsequent normal coordinate calculations.[21] On the other hand, empirical correlations of the frequencies of selected Raman lines with the porphyrin core size[22,23] or with molecular species of axial ligands[24] have also been discussed for iron-porphyrin derivatives.

For most heme enzymes the sixth coordination position of heme iron is the binding site of a reacting molecule such as oxygen, while the fifth coordination position is occupied by an amino acid residue of protein, most often by an imidazole nitrogen of a histidine residue. The state of the two axial ligands and the nature of the Fe-ligand(axial) bonds are greatly involved in the biological functions of the protein. Therefore, the

* Address correspondence to this author at the Department of Molecular Physiological Chemistry, Medical School, Osaka University, Joan-cho, Kitaku, Osaka, 560, Japan.

0002-7863/80/1502-3608$01.00/0

assignment of the Fe-ligand(axial) stretching band in the RRS of hemoproteins is a fundamental subject to be studied. The Fe-ligand(sixth) stretching mode has been observed for oxyhemoglobin (oxy-Hb),[25] nitrosylhemoglobin,[26] methemoglobins,[27] and myoglobin(Mb).[28] These lines were identified by isotope substitution of the sixth ligand. The identification of the Fe-ligand(fifth) stretching mode of hemoproteins is more difficult due to difficulty in isotope replacement.

Recently a Raman line distinguishing the two quaternary structures of Hb, namely the T (low oxygen affinity) and R states (high oxygen affinity), was found by us around 216 cm^{-1} and was assigned to the Fe-N_ϵ(His F8) stretching mode.[29] This assignment was based on the isotope frequency shift observed for the ^{54}Fe isotopic substitution of deoxy-Hb[29] and deoxy-Mb.[30] However, Kincaid et al.[31] and Desbois et al.[28] claimed that the Raman line at 216 cm^{-1} is a porphyrin mode. The former and latter groups attributed the Raman lines of deoxy-Mb at 372 and 408 cm^{-1} to the Fe-N_ϵ(His F8) stretching mode, respectively. Although the former group corrected the interpretation in agreement with us,[31] the assignment is still controversial regarding the latter group.[28] Determination of the Fe-N_ϵ(His F8) stretching Raman line is extremely important to extract structural information not only from the distinct RRS of the T- and R-state deoxy-Hb's but also from the RRS of other hemoproteins[4-14] and of whole mitochondria.[32] Accordingly, we investigated, in this study, the RRS of model compounds such as iron(II) picket-fence porphyrin and iron(II) protoporphyrin IX.

The iron(II) picket-fence porphyrin can provide an isolable, crystalline dioxygen complex.[33] When distortion of the FeN_4 core was caused because the fifth ligand had a bulky side chain, cooperativity for oxygen binding was observed, although only in the solid state.[34] The RRS of the picket-fence porphyrin in CH_2Cl_2 were previously reported by Burke et al.,[35] and the Fe-O_2 stretching band was identified. However, the Fe-N(axial) stretching band was not noticed, and, furthermore, there is no Raman data so far for crystalline picket-fence porphyrins. In this study we observed the Fe-O_2 and Fe-N(axial) stretching Raman lines both in the crystalline state and in solution for iron(II) picket-fence porphyrins having little or no steric hindrance. We confirmed our previous proposal for the assignment of the Fe-N_ϵ(His F8) stretching band by observing the frequency shifts due to the ^{54}Fe isotopic substitution and the deuteration of the axial ligand.

Experimental Section

Mesotetra($\alpha,\alpha,\alpha,\alpha$-*o*-pivalamidophenyl)porphyrin [$\alpha,\alpha,\alpha,\alpha$-$H_2(T_{piv}PP)$] was synthesized according to Collman et al.[36] The $\alpha,\alpha,\alpha,\alpha$-atropisomer was confirmed by ^1H NMR and TLC. ^{56}Fe or ^{54}Fe was incorporated into $\alpha,\alpha,\alpha,\alpha$-$H_2(T_{piv}PP)$ by reacting it with anhydrous $^{56}FeBr_2$ or $^{54}FeBr_2$ under an N_2 atmosphere at 60 °C in tetrahydrofuran containing a trace amount of pyridine (Py). The iron complex [$Fe^{III}(T_{piv}PP)Br$] thus obtained was purified with basic alumina column chromatography. $^{54}FeBr_2$ was prepared from 95% enriched ^{54}Fe powder (Rohstoff-Einfuhr) and NH_4Br.

To obtain the 1,2-dimethylimidazole (1,2-Me_2Im) complex of iron(II) picket-fence porphyrin [$Fe^{II}(T_{piv}PP)$(1,2-Me_2Im)] having a ferrous high-spin iron ($S = 2$), a hot toluene solution of $Fe^{III}(T_{piv}PP)Br$ and a fivefold excess of 1,2-Me_2Im was degassed by flushing with N_2 gas in a screw-cap septum vial, and then aqueous sodium dithionite was added to it. After the solution was vigorously shaken, the aqueous layer was removed with an air-tight syringe. To facilitate crystallization, heptane was slowly added to the solution with stirring. The crystalline complex was isolated by suction filtration, washed with heptane, and dried by evaporation. The visible spectrum of it in toluene was coincident with the reported one.[36]

As a ferrous, low-spin complex, the bis(1-methylimidazole) complex [$Fe^{II}(T_{piv}PP)$(1-MeIm)$_2$] was obtained in the same way as mentioned above except for replacement of 1,2-Me_2Im with 1-methylimidazole (1-MeIm). The crystalline samples of oxygenated complexes, namely, $Fe^{II}(T_{piv}PP)$(1-MeIm)O_2 and $Fe^{II}(T_{piv}PP)$(1,2-Me_2Im)O_2, were obtained according to Collman et al.[36] and confirmed by visible absorption spectra. All their solution samples were prepared from the crystalline complexes in a screw-cap septum cell in the presence of slight excess of axial bases (1-MeIm or 1,2-Me_2Im) under 1 atm of O_2 gas (oxy form) or under N_2 gas (deoxy form).

2-Methylimidazole (2-MeIm) was perdeuterated using the method reported by Kincaid et al.[31] and recrystallized from benzene twice. Deuteration of more than 95% of all CH groups (2-MeIm-d_5) was confirmed by ^1H NMR based on a standard signal of a known amount of Me_4Si. The 2-MeIm complex of ferrous picket-fence porphyrin [$Fe^{II}(T_{piv}PP)$(2-MeIm)] was obtained in a Raman cell by shaking vigorously the CH_2Cl_2 solution of $Fe^{III}(T_{piv}PP)Br$ overlayed with the aqueous sodium dithionite solution containing a slight excess of a given axial base (2-MeIm-h_5 or 2-MeIm-d_5).

The 2-MeIm complex of iron protoporphyrin [Fe^{II}(PP)(2-MeIm)] was derived from an aqueous solution of hemin (bovine, Sigma Type I). In the experiment involving the concentration dependence of cetyltrimethylammonium bromide (CTAB), the 10 mM solution of hemin was diluted to 0.3 mM by the aqueous CTAB solution with a given concentration, and 30 μL of aqueous 2-MeIm solution (1 M) was added to 300 μL of the CTAB-hemin solution in the Raman cell. Immediately after the addition of an extremely small amount of solid dithionite, the Raman cell was slowly evacuated to 0.1 Torr and closed. This was enough to protect the sample from autoxidation.

Raman scattering was excited by the 457.9-nm line of an Ar/Kr mixed gas laser (Spectra-Physics, Model 164) and 441.6-nm line of a He/Cd laser (Kinmon Electrics, CDR30MGH) and was recorded on a JEOL-400D Raman spectrometer. Calibration of the spectrometer was performed with indene[37] and, for the 457.9-nm excitation, with the plasma lines of the laser at 170, 188, and 257 cm^{-1}. The RRS of the solution samples were measured at 10 °C in a thermostatically controlled cell holder as usual. The RRS of solid samples were measured in a homemade cryostat. Powdered crystals were held on the sloped surface of a triangle-pillared aluminum block which was screwed to a copper block serving as the bottom of the container of the cooling medium. The pressure in the cryostat was kept at 0.05 Torr for the deoxy state, but, for the oxy state, the cryostat was filled with 1 atm of oxygen gas. Dry air was flushed against the outer front wall and bottom of the cryostat during the Raman measurements. The temperature was kept at about 220 K for the oxy state and at 77 K for the deoxy state.

Results

Figure 1 shows the RRS of $^{56}Fe^{II}(T_{piv}PP)$(2-MeIm-d_5), $^{56}Fe^{II}(T_{piv}PP)$(2-MeIm-h_5), and $^{54}Fe^{II}(T_{piv}PP)$(2-MeIm-h_5). The whole RRS of $^{56}Fe^{II}(T_{piv}PP)$(2-MeIm) above 330 cm^{-1} was coincident with the reported one,[35] but the Raman line at 209 cm^{-1} was displayed here for the first time. This line was shifted to 212 cm^{-1} on the ^{54}Fe isotope substitution and to 206 cm^{-1} on deuteration of 2-MeIm, whereas the 368-cm^{-1} line remained unshifted. The frequency shift on the ^{54}Fe isotope substitution (+3 cm^{-1}) for $^{56}Fe^{II}(T_{piv}PP)$(2-MeIm) was in good agreement with that of the 207-cm^{-1} line of Fe^{II}(PP)-(2-MeIm) (+4 cm^{-1}).[29] If the 209-cm^{-1} line were due to a pure Fe(II)-N(2-MeIm) stretching mode in which 2-MeIm moves as a whole, the expected frequency shift would be as large as 2.3 cm^{-1} for the ^{54}Fe substitution and 2.5 cm^{-1} for perdeuteration of 2-MeIm. Accordingly, the 209-cm^{-1} line is reasonably assigned to the mode primarily due to Fe(II)-N(2-MeIm) stretching vibration. This observation strongly supports our previous proposal that the quaternary structure-sensitive Raman line of deoxy-Hb arose from the Fe(II)-N_ϵ (His F8) stretching vibration.[29]

Figure 2 shows the RRS of various derivatives of $Fe^{II}(T_{piv}PP)LL'$ in CH_2Cl_2. 2-MeIm and 1-MeIm have an identical mass for the Fe(II)-N(axial) stretching mode. Stereochemically, however, the porphyrin core of $Fe^{II}(T_{piv}PP)$(2-MeIm) is distorted due to steric repulsion between the 2-CH_3 side chain and pyrrole nitrogens.[38] Consequently the bond strength of the Fe(II)-N(1-MeIm) bond without steric hindrance is presumed to be stronger than that of Fe(II)-N(2-MeIm). In accord, the Fe(II)-N(1-MeIm) stretching band

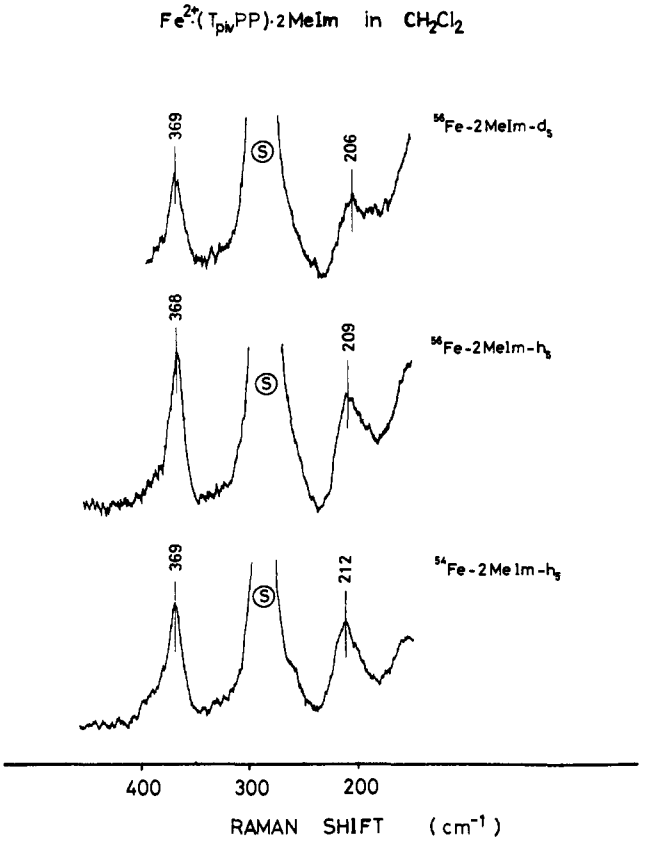

Figure 1. Resonance Raman spectra of $^{56}Fe^{II}(T_{piv}PP)$(2-MeIm-d_5), $^{56}Fe^{II}(T_{piv}PP)$(2-MeIm-h_5), and $^{54}Fe^{II}(T_{piv}PP)$(2-MeIm-h_5) in CH_2Cl_2 excited at 457.9 nm. The Raman line marked with S is due to solvent. Sample concentration: ~0.3 mM.

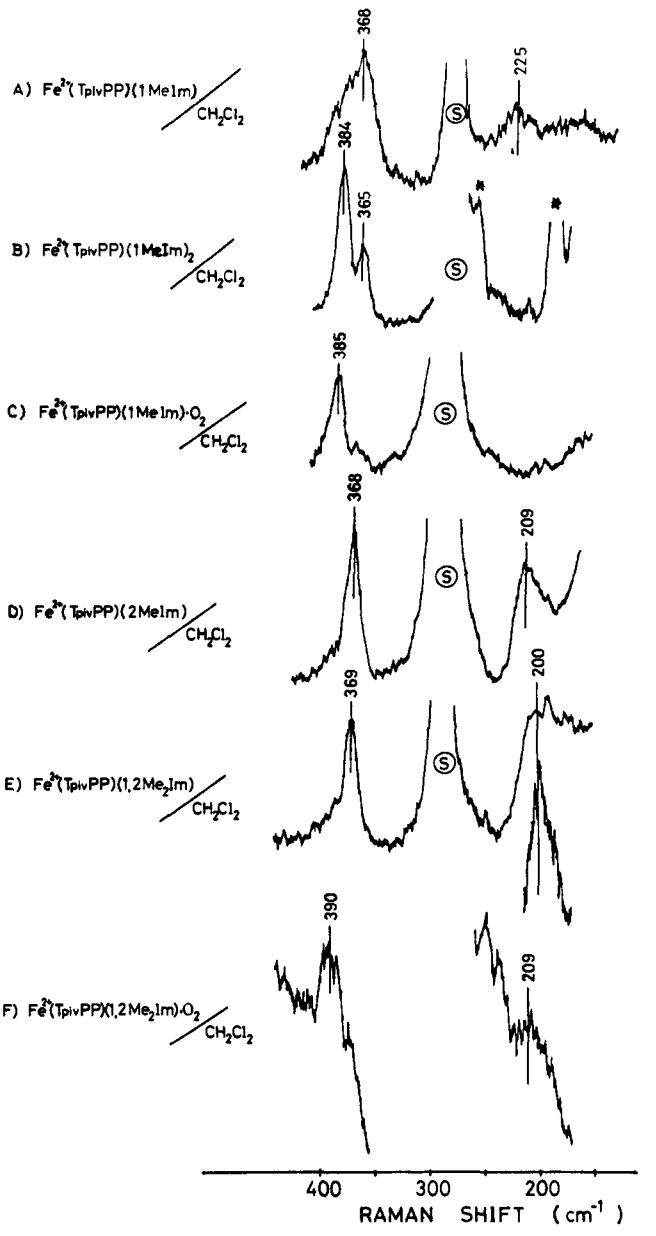

Figure 2. Resonance Raman spectra of $Fe^{II}(T_{piv}PP)LL'$ in CH_2Cl_2 solution excited at 457.9 nm. The Raman lines marked with S are due to solvent. The peaks marked with asterisks are due to the plasma line of the laser. Sample concentration: 0.2 mM. (A) L = 1-MeIm, L′ = none; (B) L = L′ = 1-MeIm; (C) L = 1-MeIm, L′ = O_2; (D) L = 2-MeIm, L′ = none; (E) L = 1,2-Me_2Im, L′ = none; (F) L = 1,2-Me_2Im, L′ = O_2; excitation, 457.9 nm. Inset of E was excited at 441.6 nm.

was observed at slightly higher frequency (225 cm^{-1}) than the Fe(II)-N(2-MeIm) stretching frequency (209 cm^{-1}). The Fe(II)-N(1-MeIm) stretching line of the five-coordinated high-spin complex disappeared for the bis(1-MeIm) complex (Figure 2B). This may possibly be overlapped with the intense solvent band at 270 cm^{-1}. A distinct difference between the mono- and bis(1-MeIm) complexes is seen in the appearance of a new band at 384 cm^{-1} for the latter. $Fe^{II}(T_{piv}PP)$(1-MeIm)O_2 also showed a Raman line at 385 cm^{-1}, but the Fe(II)-N(1-MeIm) stretching was not observed (Figure 2C).

$Fe^{II}(T_{piv}PP)$(1,2-Me_2Im) is inferred to adopt the five-coordinated ferrous high-spin states as $Fe^{II}(T_{piv}PP)$(2-MeIm), but the effective mass of the axial ligand differed between them. The Fe(II)-N(1,2-Me_2Im) stretching band would be shifted by 6.3 cm^{-1} from the Fe(II)-N(2-MeIm) stretching band provided that their force constants were identical. In fact, $Fe^{II}(T_{piv}PP)$(1,2-Me_2Im) gave a Raman line at 200 cm^{-1}, which was obscure upon excitation of 457.9 nm but evident at 441.6 nm (Figure 2E). On oxygenation of $Fe^{II}(T_{piv}PP)$(1,2-Me_2Im), the Fe(II)-N(1,2-Me_2Im) stretching line moved to 209 cm^{-1}, though broad, and simultaneously the 369-cm^{-1} line was replaced by the 390-cm^{-1} line (Figure 2F) in the same way as the case of $Fe^{II}(T_{piv}PP)$(1-MeIm) (see spectra A and C in Figure 2). Apparently the presence of a Raman line around 384-390 cm^{-1} or 365-370 cm^{-1} corresponds to the ferrous low-spin or high-spin state, respectively, as Burke et al. pointed out.[35]

Figure 3 compares the Fe-O_2 stretching bands of Fe^{II}-$(T_{piv}PP)$(1-MeIm)O_2 (A) and $Fe^{II}(T_{piv}PP)$(1,2-Me_2Im)O_2 (B) between solid and solution states. Oxygenation was monitored by the so-called "oxidation state marker" (ν_4),[21] which appeared at 1365 and 1355 cm^{-1} for the oxy and deoxy states of $Fe^{II}(T_{piv}PP)$(1-MeIm) in CH_2Cl_2, respectively. The Raman line of $Fe^{II}(T_{piv}PP)$(1-MeIm)O_2 in CH_2Cl_2 at 568 cm^{-1} was previously identified as the Fe-O_2 stretching Raman line by Burke et al.[35] and in fact disappeared on deoxygenation. For the solid state, the ν_4 lines of the oxy and deoxy forms were observed at the same frequency as for the solution. However, the Fe-O_2 stretching line was observed at appreciably lower frequencies in the solid state (555 cm^{-1}) than in solution (568 cm^{-1}).

The ν_4 line of $Fe^{II}(T_{piv}PP)$(1,2-Me_2Im) with appreciable steric hindrance[34] was observed at 1365 and 1345 cm^{-1} for the oxy and deoxy states in CH_2Cl_2, respectively, as shown in Figure 3B. The latter frequency was definitely lower than that of $Fe^{II}(T_{piv}PP)$(1-MeIm). However, the Fe-O_2 stretching band was observed at the same frequency (568 cm^{-1}) as that of $Fe^{II}(T_{piv}PP)$(1-MeIm)O_2 having no steric hindrance. The ν_4 frequencies were the same for the solid state and solution,

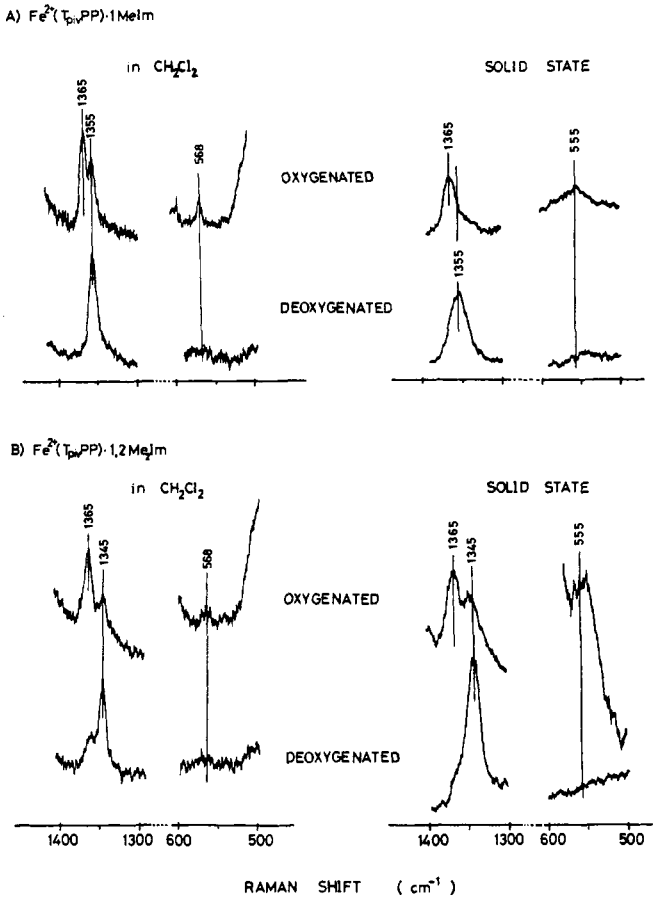

Figure 3. Resonance Raman spectra of $Fe^{II}(T_{piv}PP)$(1-MeIm), $Fe^{II}(T_{piv}PP)$(1-MeIm)O_2, $Fe^{II}(T_{piv}PP)$(1,2-Me_2Im), and $Fe^{II}(T_{piv}PP)$-(1,2-Me_2Im)O_2 in the ν_4 and Fe-O_2 stretching regions. Left side, in CH_2Cl_2 solution (0.5 mM); right side, in solid state: (A) $Fe^{II}(T_{piv}PP)$-(1-MeIm); (B) $Fe^{II}(T_{piv}PP)$(1,2-Me_2Im).

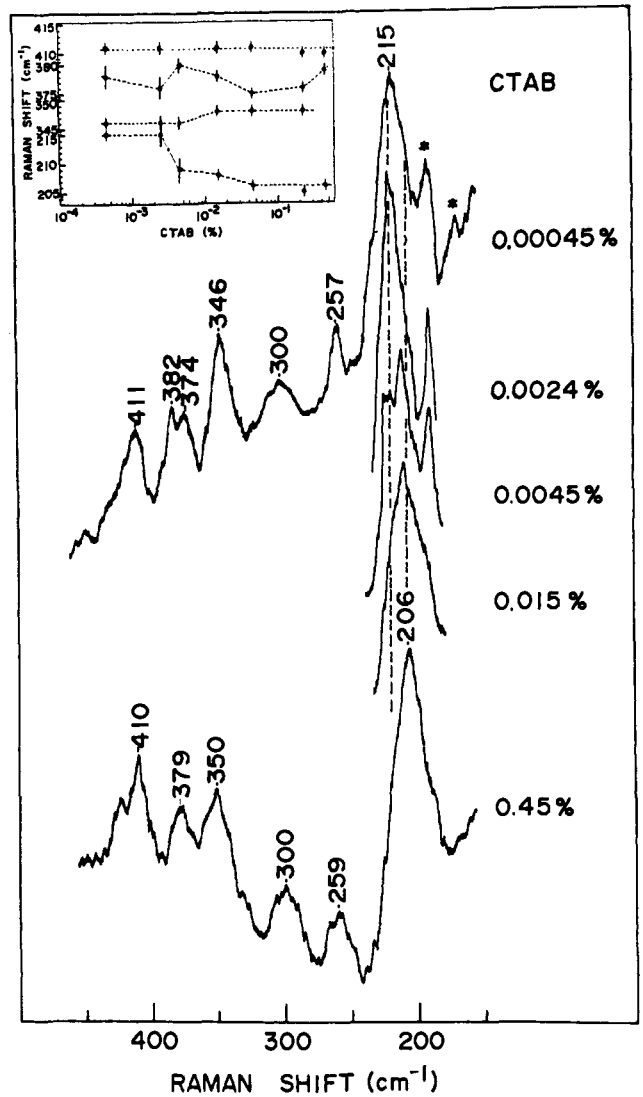

Figure 4. Dependence of the resonance Raman spectra of Fe^{II}(PP)(2-MeIm) in aqueous solution on the concentrations of CTAB. The concentration of CTAB (w/w) is specified at the right side of individual spectra. In an inset figure, the apparent peak frequencies (main peak) of selected Raman lines are plotted against the concentration of CTAB. The concentration of porphyrin is kept at 0.3 mM; excitation, 457.9 nm.

although oxygenation was incomplete due to lower oxygen affinity of this complex. The Fe-O_2 stretching mode of solid $Fe^{II}(T_{piv}PP)$(1,2-Me_2Im)O_2 was identified at 555 cm^{-1}, since this line disappeared completely when the oxygen pressure was reduced. We failed to detect the Fe-N(ligand) stretching band for the solid state because of strong tailing of very intense Rayleigh scattering.

The Fe-N(2-MeIm) stretching mode of Fe^{II}(PP)(2-MeIm) was previously reported at 207 cm^{-1} by us, but at 220 cm^{-1} by Kincaid et al.[31] The discrepancy is serious and should be clarified. Salmeen et al.[12] pointed out the phenomenon of molecular aggregation for heme *a*-bisimidazole complexes, which was avoided in the presence of detergent. As our previous measurements were performed in the presence of CTAB, we examined the dependence of that frequency upon the CTAB concentration. As shown in Figure 4, the Fe-N(2-MeIm) stretching mode was observed at 206 and 215 cm^{-1} in the presence of 0.45 and 0.000 45% CTAB (w/w), respectively. Around 0.0045% CTAB, both lines were observed and, therefore, the existence of two kinds of states is evident. Since estimation of the relative intensities of the two bands was difficult because of overlapping, the apparent peak frequencies were plotted against the concentration of CTAB in an inset of Figure 4, where the frequencies of a few selected peaks were also plotted. The doublet-like appearance of the 379-cm^{-1} line for a dilute solution of CTAB agreed with the spectrum of Figure 1 of ref 31 measured for the solution without CTAB. Thus, the apparent discrepancy between the two reports[29,31] was determined to be caused by the presence of detergent.

The 220-cm^{-1} band of the Fe-N(2-MeIm) stretching vibration in the absence of detergent is close to the N-Fe-N symmetric stretching mode of Fe^{II}(PP)$(Im)_2$ at 225 cm^{-1}.[29] However, the possibility of bis(2-MeIm) complex formation is ruled out because, when the ratio of 2-MeIm/Fe^{II}(PP) was varied from 54 to 1088 in the absence of CTAB, the Raman lines at 221, 303, and 380 cm^{-1} were continuously shifted to 217, 298, and 377 cm^{-1}, respectively. This spectral change distinctly differed from that for increasing concentrations of CTAB. Therefore, we tentatively assume that micelle formation of CTAB cuts off interactions of 2-MeIm with solvent such as the H_2O···H-N(3)(2-MeIm) hydrogen bond, causing a slight change in the electronic state of 2-MeIm and thus of the Fe(II)-N(2-MeIm) bond strength. Subsequently, the appearance of the CTAB-induced large frequency change only in the Fe(II)-N(2-MeIm) stretching mode becomes understandable.

The RRS of Fe^{II}(PP)(2-MeIm-h_5) and Fe^{II}(PP)(2-MeIm-d_5) in 0.25% CTAB solution was shown in Figure 5. The Raman line of Fe^{II}(PP)(2-MeIm-h_5) at 206 cm^{-1} exhibited a frequency shift by -3 cm^{-1} upon deuteration of 2-MeIm, in good agreement with the results for $Fe^{II}(T_{piv}PP)$-(2-MeIm) shown in Figure 1. The Raman lines at 377 and 410 cm^{-1}, previously proposed as the Fe(II)-N(ligand) stretching band,[28,31] did not show such frequency shifts. The 206-cm^{-1}

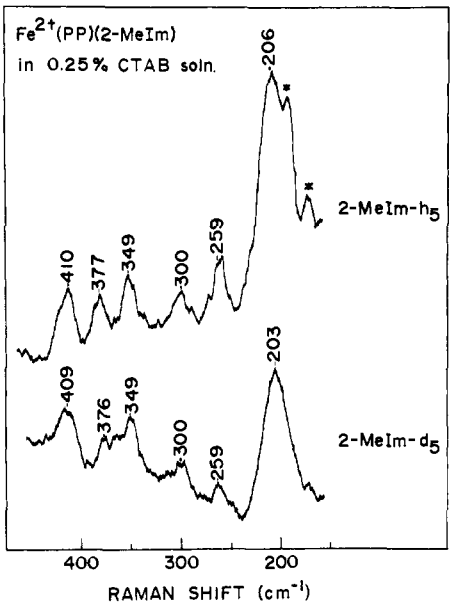

Figure 5. Comparison of the resonance Raman spectrum of Fe^{II}(PP)(2-MeIm-h_5) and Fe^{II}(PP)(2-MeIm-d_5) in 0.25% CTAB (w/w) aqueous solution. The concentration of porphyrin is 0.3 mM and that of 2-MeIm is about 50 mM; excitation, 457.9 nm.

line showed a frequency shift by +4 cm^{-1} upon ^{54}Fe isotopic substitution.[29] All these data evidently indicated that the 206-cm^{-1} line of Fe^{II}(PP)(2-MeIm) and the 209-cm^{-1} line of $Fe^{II}(T_{piv}PP)$(2-MeIm) are most significantly associated with the Fe(II)-N(2-MeIm) stretching vibration.

Discussion

Assignment of the Fe-N(2-MeIm) Stretching Band. The discovery of the quaternary structure-sensitive Raman line of deoxy-Hb[29] at 216 cm^{-1} has made the assignment of this line extremely important. The experimental results on isotopic substitutions of Fe of deoxy-Hb[29] and deoxy-Mb[30] as well as on isotope substitutions of Fe and 2-MeIm of $Fe^{II}(T_{piv}PP)$(2-MeIm) and Fe^{II}(PP)(2-MeIm) positively indicated that the Raman line arose from the Fe(II)-N(ligand) stretching mode. Theoretical consideration for the RRS of two different types of porphyrins ($T_{piv}PP$ and PP) also supports the assignment.

According to the normal coordinate calculations of Ni(OEP),[21] the lowest frequency, totally symmetric mode [ν_9, 230 cm^{-1} for Ni(OEP)] involves primarily the C_β-C(peripheral) bending coordinate (23%). As $Fe^{II}(T_{piv}PP)$(2-MeIm) has only C_β-H bonds but no C_β-C(peripheral) bonds, the ν_9 frequency should differ between $Fe^{II}(T_{piv}PP)$(2-MeIm) and Fe^{II}(PP)(2-MeIm). The lowest frequency B_{1g} mode [ν_{18}, 187 cm^{-1} for Ni(OEP)] involves the $C_\alpha C_m C_\alpha$ bending character (39%).[21] Because of the very different C_m substituents (H for PP and the *o*-pivalamidophenyl group for $T_{piv}PP$), the ν_{18} frequency should also differ between the two types of porphyrins. The same is true for the lowest and next lowest B_{2g} modes [ν_{35} and ν_{34}, expected at 182 and 232 cm^{-1}, respectively, for Ni(OEP)].[21] There is no other porphyrin mode responsible for the Raman lines below 250 cm^{-1}. For the Raman lines in question [209 cm^{-1} for $Fe^{II}(T_{piv}PP)$(2-MeIm) and 206 cm^{-1} for Fe^{II}(PP)(2-MeIm)], invariance of their frequencies between the two different types of porphyrins precludes assigning them to one of the porphyrin modes.

Recently, Wright et al.[39] demonstrated that the N-Fe(II)-N symmetric stretching mode of bispyridine iron(II) mesoporphyrin dimethyl ester was located at 179 cm^{-1} and that the line was more intensified at the charge-transfer band between Py and Fe(II) presumed at 496.5 nm. This frequency is in reasonable agreement with the present assignment in taking the different coordination number and different character of chemical bonds into consideration. Furthermore, the coincidence of the Fe-O_2 stretching frequency between oxy-Hb[25,29] and $Fe^{II}(T_{piv}PP)(1,2\text{-}Me_2Im)O_2$ in CH_2Cl_2[35] would allow us to deduce that the Fe-N(fifth ligand) stretching force constants of both compounds are alike even in the deoxy state. Consequently, it is concluded that the 216-cm^{-1} line of deoxy-Hb[29] and the 220-cm^{-1} line of deoxy-Mb[30] as well as the 206-cm^{-1} line of Fe^{II}(PP)(2-MeIm) and the 209-cm^{-1} line of $Fe^{II}(T_{piv}PP)$(2-MeIm) are all associated mainly with the Fe(II)-N(fifth ligand) stretching vibration. The recent observation of the quaternary structure-linked distinct frequency shifts of the α^{deoxy} or β^{deoxy} subunit of valency hybrid hemoglobin for the 216-cm^{-1} line[40] then implies different structural distortions of the Fe-N_ϵ(His F8) bonds of the α and β subunits.

The vibrational displacements of the Fe(II) ion and 2-MeIm group as a whole during the Fe-ligand stretching motion can be calculated from the observed isotope shift and eq 1:[41]

$$\langle X_\alpha^2 \rangle_T = \frac{h(\nu_0 + \nu_\alpha)}{8\pi^2 \nu_0^3 c} \frac{\Delta\nu_\alpha}{\Delta m_\alpha} \frac{m_\alpha}{m_{0\alpha}} \frac{1 + \exp(-h\nu_0/kT)}{1 - \exp(-h\nu_0/kT)} \quad (1)$$

where X_α is a root-mean-square displacement of the αth atom, ν_0 and ν_α are the frequencies of the parent and isotope substituted molecules, $m_{0\alpha}$ and m_α are masses of the nonlabeled and labeled αth atom, Δm_α is a mass difference ($= m_{0\alpha} - m_\alpha$), and $\Delta\nu_\alpha$ is the isotopic frequency shift. For α = Fe (ν_0 = 209 and ν_α = 212 cm^{-1}) and α = 2-MeIm (ν_0 = 209 cm^{-1} and ν_α = 206 cm^{-1}), numerical calculation gave rise to $X_{Fe} = 0.04_8$ and $X_{2\text{-MeIm}} = 0.03_1$ Å at 10 °C, respectively. Those values correspond to the mean amplitude for the motion of the Fe and N atoms perpendicular to the porphyrin plane. The Fe(II)-N(2-MeIm) stretching force constant is calculated to be 0.85 mdyn/Å, close to the Ni(II)-N(pyrrole) stretching force constant (0.7 mdyn/Å) used for the normal coordinate calculations.[21]

Cooperativity for Oxygen Binding. Collman et al.[34] demonstrated that $Fe^{II}(T_{piv}PP)$(2-MeIm) and $Fe^{II}(T_{piv}PP)$-(1,2-Me_2Im) display sigmoidal curves for oxygen binding, but $Fe^{II}(T_{piv}PP)$(1-MeIm) shows a linear curve. The cooperativity was observed only for the solid state. Accordingly, Fe^{II}-($T_{piv}PP$)(1,2-Me_2Im) and $Fe^{II}(T_{piv}PP)$(1-MeIm) in the solid state are considered to serve as a model for the T and R states of deoxy-Hb, respectively. In relation to the Raman spectral difference between the T and R states of deoxy-Hb,[29] comparison of the RRS of $Fe^{II}(T_{piv}PP)$(1,2-Me_2Im) and Fe^{II}-($T_{piv}PP$)(1-MeIm) is interesting.

The ν_4 frequency differed between the two complexes only in the deoxy state. The ν_4 frequency is considered to reflect π basicity of the fifth ligand;[42,43] the lower the frequency is, the higher the π basicity. Accordingly, 1,2-Me_2Im may have higher π basicity than 1-MeIm when they were bound to the fifth coordination position of the heme iron. It must be stressed, however, that the frequency difference was preserved in CH_2Cl_2 (see Figure 3) and, therefore, would not be essential to the cooperative oxygen binding. Presumably the lower ν_4 frequency is related to the lower oxygen affinity [$p_{1/2}$ = 38 Torr for $Fe^{II}(T_{piv}PP)$(1,2-Me_2Im) and $p_{1/2}$ = 0.3 Torr for $Fe^{II}(T_{piv}PP)$(1-MeIm) in toluene].[34]

It was noted in Figure 3 that the Fe-O_2 stretching frequencies of these two kinds of complexes were identical. This implies that, although the oxygen affinity may be manipulated by the steric factor of the fifth ligand, the Fe-O_2 bond energy after oxygenation is little affected by such a factor. This fact is in good agreement with the conclusion for oxy-Hb[29] that the Fe-O_2 bond energy is unaltered by the change of quaternary structure. Such a lack of correlation between oxygen affinity and the Fe-O_2 stretching frequencies was recently confirmed

for Mb's reconstituted with formyl hemes.[44] Therefore, it is likely that the free energy of cooperation for oxygen binding of Hb arises primarily from an energy difference between the T and R states of deoxy states.

The $Fe-O_2$ stretching frequency of the model compounds in CH_2Cl_2 (568 cm^{-1}) and that of oxy-Hb (567 cm^{-1}) showed remarkable coincidence as pointed out first by Burke et al.[35] On the other hand, the $Fe-O_2$ stretching frequencies of the model compounds in the solid state (555 cm^{-1}) were clearly lower than those for the CH_2Cl_2 solution irrespective of the presence of the steric hindrance at the trans position (Figure 3). This indicates the presence of some interaction between bound oxygen and the adjacent porphyrin group in the crystal lattice. The interaction may have transmitted the oxygen binding of a given molecule to the adjacent molecule in the same unit cell, most probably to its axial ligand, resulting in the appearance of the cooperativity.

In conclusion, the Raman line of deoxy-Hb A at 216 cm^{-1}, which is shifted to 220 cm^{-1} on transition to the R state,[29] is now assigned to the $Fe-N_\epsilon$(His F8) stretching mode. The Fe-N(ligand) stretching and ν_4 frequencies differed between $Fe^{II}(T_{piv}PP)$(2-MeIm) and $Fe^{II}(T_{piv}PP)$(1-MeIm), but the $Fe-O_2$ stretching and ν_4 frequencies did not differ between $Fe^{II}(T_{piv}PP)(1,2\text{-}Me_2Im)O_2$ and $Fe^{II}(T_{piv}PP)(1\text{-}MeIm)O_2$ even in the solid state. Accordingly, it was inferred that oxygen affinity of the model hemes as well as of hemoglobin depends primarily upon the deoxy state.

Acknowledgments. The authors express their gratitude to Dr. Hideki Morimoto of Osaka University and Dr. Kiyoshi Nagai of Nara Medical College for stimulating discussions. They also thank Kinmon Electric Corp. for the use of a He/Cd laser.

References and Notes

(1) T. G. Spiro, *Biochim. Biophys. Acta*, **416**, 169–187 (1975).
(2) R. H. Felton and N.-T. Yu, in "The Porphyrins", D. Dolphin, Ed., Vol. 3, Academic Press, New York, 1978, Chapter 8.
(3) T. Kitagawa, Y. Ozaki, and Y. Kyogoku, *Adv. Biophys.*, **11**, 153–192 (1978).
(4) (a) P. M. Champion and I. C. Gunsalus, *J. Am. Chem. Soc.*, **99**, 2000–2002 (1977); (b) P. M. Champion, I. C. Gunsalus, and G. C. Wagner, *ibid.*, **100**, 3743–3751 (1978).
(5) (a) Y. Ozaki, T. Kitagawa, Y. Kyogoku, H. Shimada, T. Iizuka, and Y. Ishimura, *J. Biochem. (Tokyo)*, **80**, 1447–1451 (1976); (b) Y. Ozaki, T. Kitagawa, Y. Kyogoku, Y. Imai, C. Hashimoto-Yutsudo, and R. Sato, *Biochemistry*, **17**, 5826–5831 (1978).
(6) G. Rakshit and T. G. Spiro, *Biochemistry*, **13**, 5317–5323 (1974).
(7) R. H. Felton, A. Y. Romans, N.-T. Yu, and G. R. Schonbaum, *Biochim. Biophys. Acta*, **434**, 82–89 (1976).
(8) R. D. Champion, P. M. Champion, D. B. Fitchen, R. Chiang, and L. P. Hager, *Biochemistry*, **18**, 2280–2290 (1979).
(9) T. C. Strekas and T. G. Spiro, *Biochim. Biophys. Acta*, **351**, 237–245 (1974).
(10) T. Kitagawa, Y. Ozaki, Y. Kyogoku, and T. Horio, *Biochim. Biophys. Acta*, **495**, 1–11 (1975).
(11) F. Adar and T. Yonetani, *Biochim. Biophys. Acta*, **502**, 80–86 (1978).
(12) I. Salmeen, L. Rimai, and G. T. Babcock, *Biochemistry*, **17**, 800–806 (1978).
(13) G. T. Babcock and I. Salmeen, *Biochemistry*, **18**, 2493–2498 (1979).
(14) T. Kitagawa and Y. Orii, *J. Biochem. (Tokyo)*, **84**, 1245–1252 (1978).
(15) H. Ogoshi, Y. Saito, and K. Nakamoto, *J. Chem. Phys.*, **57**, 4194–4202 (1972).
(16) S. Sunder and H. Bernstein, *J. Raman Spectrosc.*, **5**, 351–371 (1976).
(17) H. Susi and J. S. Ard, *Spectrochim. Acta, Part A*, **33**, 561–567 (1977).
(18) P. Stein, J. M. Burke, and T. G. Spiro, *J. Am. Chem. Soc.*, **97**, 2304–2305 (1975).
(19) M. Abe, T. Kitagawa, and Y. Kyogoku, *Chem. Lett.*, 249–252 (1976).
(20) (a) T. Kitagawa, M. Abe, and H. Ogoshi, *J. Chem. Phys.*, **69**, 4516–4525 (1978); (b) T. Kitagawa, M. Abe, Y. Kyogoku, H. Ogoshi, H. Sugimoto, and Z. Yoshida, *Chem. Phys. Lett.*, **48**, 55–58 (1977).
(21) M. Abe, T. Kitagawa, and Y. Kyogoku, *J. Chem. Phys.*, **69**, 4526–4534 (1978).
(22) (a) R. H. Felton, N.-T. Yu, D. C. O'Shea, and J. A. Shelnutt, *J. Am. Chem. Soc.*, **96**, 3675–3677 (1974); (b) L. D. Spaulding, C. C. Chang, N.-T. Yu, and R. H. Felton, *ibid.*, **97**, 2517–2524 (1975).
(23) T. G. Spiro, J. D. Stong, and P. Stein, *J. Am. Chem. Soc.*, **101**, 2648–2655 (1979).
(24) J. Teraoka and T. Kitagawa, *J. Phys. Chem.*, in press.
(25) H. Brunner, *Naturwissenschaften*, **61**, 129–130 (1974).
(26) G. Chottard and D. Mansuy, *Biochem. Biophys. Res. Commun.*, **77**, 1333–1338 (1977).
(27) S. A. Asher, L. E. Vickery, T. M. Shuster, and K. Sauer, *Biochemistry*, **16**, 5849–5856 (1977).
(28) A. Desbois, M. Lutz, and R. Banerjee, *Biochemistry*, **18**, 1510–1518 (1979).
(29) K. Nagai, T. Kitagawa, and H. Morimoto, *J. Mol. Biol.*, **136**, 271–289 (1980).
(30) T. Kitagawa, K. Nagai, and M. Tsubaki, *FEBS Lett.*, **104**, 376–378 (1979).
(31) J. Kincaid, P. Stein, and T. G. Spiro, *Proc. Natl. Acad. Sci. U.S.A.*, **76**, 549–552, 4156 (1979).
(32) (a) F. Adar and M. Erécinska, *Biochemistry*, **17**, 5484–5488 (1978); (b) *ibid.*, **18**, 1825–1829 (1979).
(33) J. P. Collman, R. R. Gagne, C. A. Reed, W. T. Robinson, and G. A. Rodley, *Proc. Natl. Acad. Sci. U.S.A.*, **71**, 1326–1329 (1974).
(34) J. P. Collman, J. I. Brauman, E. Rose, and K. S. Suslick, *Proc. Natl. Acad. Sci. U.S.A.*, **75**, 1052–1055 (1978).
(35) J. M. Burke, J. R. Kincaid, S. Peters, R. R. Gagne, J. P. Collman, and T. G. Spiro, *J. Am. Chem. Soc.*, **100**, 6083–6088 (1978).
(36) J. P. Collman, R. R. Gagne, C. A. Reed, T. R. Halbert, G. Lang, and W. T. Robinson, *J. Am. Chem. Soc.*, **97**, 1427–1439 (1975).
(37) P. J. Hendra and E. J. Loader, *Chem. Ind. (London)*, 718–719 (1961).
(38) J. P. Collman and C. A. Reed, *J. Am. Chem. Soc.*, **95**, 2048–2049 (1973).
(39) P. G. Wright, P. Stein, J. M. Burke, and T. G. Spiro, *J. Am. Chem. Soc.*, **101**, 3531–3535 (1979).
(40) K. Nagai and T. Kitagawa, *Proc. Natl. Acad. Sci. U.S.A.*, in press.
(41) T. Miyazawa, *J. Mol. Spectrosc.*, **13**, 321–325 (1964).
(42) T. Kitagawa, Y. Kyogoku, T. Iizuka, and M. I. Saito, *J. Am. Chem. Soc.*, **98**, 5169–5173 (1976).
(43) T. G. Spiro and J. M. Burke, *J. Am. Chem. Soc.*, **98**, 5482–5489 (1976).
(44) M. Tsubaki, K. Nagai, and T. Kitagawa, *Biochemistry*, **19**, 379–385 (1980).